Compositions of early Islamic glass along the Iranian Silk Road

Nadine Schibille, James W Lankton, Bernard Gratuze

Geochemistry xxx (xxxx) xxx

Contents lists available at ScienceDirect

Geochemistry

journal homepage: www.elsevier.com/locate/chemer

Compositions of early Islamic glass along the Iranian Silk Road

Nadine Schibille [a,*], James W. Lankton [b], Bernard Gratuze [a]

[a] Institut de recherche sur les archéomatériaux, Centre Ernest-Babelon (IRAMAT-CEB), UMR7065, CNRS/Université d'Orléans, 45071 Orléans, France
[b] Institute of Archaeology, University College, London, UK

ARTICLE INFO

Handling Editor: Vincenza Guarino

Keywords:
Islamic glass
Iran
Plant ash glass
Chromium
Thorium
Zirconium
Samarra
Merv
Nishapur

ABSTRACT

The composition of archaeological glass reflects the geochemical nature of its raw materials. To determine the origins and distribution of early Islamic glasses from Iran, a set of 169 glass samples from five different sites was analysed by laser ablation inductively coupled plasma mass spectrometry (LA-ICP-MS) of 58 elements. The glasses were classified into six different plant ash glass groups, three of which were attributed to a Mesopotamian origin, while three further groups are presumed to represent regional Iranian productions. The ratios of MgO/CaO and K_2O/P_2O_5 of the different groups reflect variations in the plant ash component. Minor elements Cr, Ti, Zr, La and Th and their ratios proved effective in distinguishing the base glass types. Mapping their frequency across the Iranian plateau revealed the relative movement of glass and likely source areas. The decline in the frequency of glass types with elevated Cr/La ratios east of the Zagros Mountain range confirms that elevated Cr/La ratios together with an augmentation of the magnesium levels are features of Mesopotamian glass production apparently inherited from the geochemical environment of the Euphrates and Tigris river valleys. Some exceptionally clean Mesopotamian glasses made from a quartz-rich silica with low levels of accessory minerals are consistent with ninth-century glass from Samarra, which was evidently traded widely along the Silk Road network. No evidence of local glass production was detected in Nishapur. The Iranian groups were produced from a quartz-rich silica source, high in thorium but with different zirconium contents resulting in different Th/Zr ratios. Aluminium concentrations tend to increase from west to east, with the highest values found among glass assemblages from Central Asia.

1. Introduction

The *Brill Scientific Research Collection* (BSRC) at the Corning Museum of Glass includes early Islamic glass from various locations in Iran, acquired by the museum from Ray Winfield Smith between the 1950s through to the late 1970s (Larson, 2021). Some of these fragments have been analysed by Robert Brill over the years and published in his three-volume monograph (Brill, 1999; Brill and Stapleton, 2012). Among the samples were 44 glass finds from Nishapur in north-eastern Iran dating from the ninth to the tenth century CE (Fig. 1). These formed the basis for Robert Brill's identification of an exceptional colourless glass type that he also discovered at Fustat (Egypt) and Qasr al-Hayr (Syria) (Brill, 1995), and which has since been recorded at sites throughout the Islamic world, from Spanish Córdoba in the West (De Juan Ares et al., 2021) to Samarra in Iraq in the East, where this type of clean colourless glass is now thought to have originated (Schibille et al., 2018; Wypyski, 2015). Brill's compositional data were obtained by atomic absorption spectrometry for major and minor elements, and semi-quantitative emission spectrographic analyses were carried out for trace elements (Brill, 1995). Scientific methods for analysing archaeological materials have improved considerably over the last three decades, allowing a more fine-grained characterisation of group structures and geographical attributions of first millennium glass. Recent attempts to unravel early Islamic plant ash glass groups using trace element data of glass assemblages from sites across the Near East, Mesopotamia and Iran are beginning to reveal compositional features for different geographical production zones in the Middle East (Henderson et al., 2016; Phelps, 2017; Schibille, 2022; Swan et al., 2017).

In spite of the increasing volume of data on the composition of plant ash glass from the early Islamic period, little is still known about Iranian glass and how it differs from glass produced in other Islamic regions such as Mesopotamia or the Levant. The glass from Nishapur (Brill, 1995; Henderson et al., 2016; Wypyski, 2015) and Siraf (Swan et al., 2017) are the exception, as is a recent comparative study of a small number of glass finds from the National Museum in Iran (Salehvand et al., 2020). We therefore decided to re-analyse some of Brill's samples from five

* Corresponding author.
E-mail address: nadine.schibille@cnrs.fr (N. Schibille).

https://doi.org/10.1016/j.chemer.2022.125903
Received 9 June 2022; Received in revised form 3 August 2022; Accepted 4 August 2022
Available online 8 August 2022

Fig. 1. Map of Mesopotamia and central Iran, showing the main historic Silk Routes across Eurasia (red traces) and main sites discussed in the paper highlighted in red. Created using worldmap from ArcGIS hosted by Esri, USGS (https://worldmap.maps.arcgis.com/apps/mapviewer/index.html). Layers used by StoryMaps. (For interpretation of the references to colour in this figure legend, the reader is referred to the web version of this article.)

different early Islamic sites in Iran using laser ablation inductively coupled mass spectrometry (LA-ICP-MS). The primary objective was to better understand differences in the glass compositions along the Iranian Silk Roads and to make use of minor and trace element patterns as evidence of regional glass production activities. We present new LA-ICP-MS data and map the frequency distribution of the different compositional groups that we identify from Hamadan in the west through Qom, Rayy and Gorgan to Nishapur in the east over a distance of about 1000 km (Fig. 1). The samples were selected and dated to the eighth to twelfth centuries based on typology and comparative material by Selim Abdul-Hak who later became the director of the National Museum in Damascus. No compositional differences could be detected in the four assemblages over time. We therefore concentrate on the characterisation of the glass groups and a spatial comparison as a starting point to identify diagnostic features and to postulate possible production zones for different base glass types.

The detection and quantification of differences between sites hinges on group properties rather than individual samples, and the success of this approach depends necessarily on the sample size. The larger the dataset (i.e. assemblages) the more reliable are the conclusions that can be drawn, and allowances must be made for differences in sample size when comparing data. This is relevant to the present study, where there is an almost five-fold difference in the number of data between the smallest assemblage under consideration from Hamadan and the largest collection of samples from Gorgan. However, by expressing group structures as percentages of the total number of samples in the assemblage of each site, we are able to propose a regional production model of early Islamic glass in Iran.

2. Materials and methods

2.1. Contexts and samples

169 individual glass samples were analysed, mostly vessel fragments, but also some beads and five pieces of glass working waste from Gorgan (Supplementary Table S1; Fig. 2). In addition to the samples already analysed by Robert Brill (Brill, 1995, 1999), we included previously unpublished material from the *Brill Scientific Research Collection*. The samples are from five urban centres that lie on the main arteries of the Silk Road network (Fig. 1).

Furthest west is the ancient city of **Hamadan** in the fertile plain of the upper Qareh Su River. The city was captured by the Arabs in 641 or 642 CE and served as a provincial capital until the twelfth century when Hamadan was made the capital of the Seljuq Turkish sultanate (Frye, 2012). The samples from Hamadan (n = 14) appear to date to the tenth to eleventh century and include colourless and weakly coloured samples as well as black, blue and green vessel fragments and a large mosaic eye bead with different colours (Fig. 2). Naturally-coloured vessel fragments (n = 17) were analysed from the city of **Qom** some 250 km to the east of Hamadan and about 150 km south of Tehran that date to the eighth to eleventh centuries. An important Shi'ite religious centre, Qom seems to have enjoyed a certain economic prosperity during the Seljuq period probably due to it being an important pilgrimage site and because of its famous *madrasas* (Drechsler, 2009). The archaeological site of **Rayy**, now absorbed by modern Teheran (Fig. 1), is located in a fertile zone on one of the major arteries of the Silk Road (Rante, 2008, 2015). Twenty different glass vessels plus a single bead (Fig. 2) were analysed from Rayy (n = 21).

Fig. 2. Beads, vessels and working debris with sample numbers and glass compositional types. The stratified (NIS 5335) and mosaic eye bead (HAM 5346) illustrate two techniques used during the early Islamic period, while RAY BC 02 is a compositional outlier and morphologically more similar to beads from the Achaemenid period. Glass working waste from Gorgan (GOR BC 03, GOR BC 30 and GOR BC 29, all group G2) suggests local vessel production if not local or regional primary glassmaking, in contrast to the fragments of finished vessels and beads found at Nishapur, Qom, Rayy and Hamadan.

The largest collection of samples for the present study (n = 61), comprising a wide range of different vessel fragments and five pieces of glass working waste, was recovered from **Gorgan** (Figs. 2, S2), close to the south-eastern corner of the Caspian Sea. Excavations in the 1970s yielded not only large quantities of glass but apparently also the remains of two glass furnaces that the archaeologists dated to the eleventh to twelfth century CE (Kiani, 1984; Salehvand et al., 2020). Part of the province of Khorasan during the Sasanian period, Gorgan formed a separate unit during the early Islamic period (Bosworth and Blair, 2012). The plain of Gorgan seems to have been a fertile agricultural region and, according to early Islamic textual sources, an important centre for the production of raw silk and silk textiles that were exported as far as Yemen (Bosworth, 2012).

During the ninth to thirteenth centuries, **Nishapur** was one of the most important economic and commercial centres of the province of Khorasan in north-eastern Iran. A key player in the Abbasid uprising in 748 CE, Nishapur became the Tahirid capital in the ninth century (821–873 CE), replacing Merv as capital of the autonomous province of Khorasan (Collinet, 2015; Kröger, 1995). The affluence of Nishapur was a result of trade and the presence of abundant natural resources (Holakooei et al., 2018). The main industry was the production of cotton textiles and Nishapur supplied a vast and growing market (Bulliet, 2009, 2018). Between 1935 and 1940, the Persian (later Iranian) expedition of the Metropolitan Museum of Art carried out several excavations at Nishapur, concentrating particularly on the area of the Tepe Madraseh' and the Tepe Sabz Pushan, from which the majority of the materials including glass comes (Hauser and Wilkinson, 1942; Wilkinson, 1973). It has been assumed ever since that glass must have been produced in Nishapur, even though there is no archaeological evidence to support this hypothesis (Collinet, 2015; Hauser and Wilkinson, 1942; Kröger, 1995). For the present study, we re-analysed all 44 of Brill's samples, some of which are now in the Metropolitan Museum of Art in New York. They were attributed to the ninth to tenth centuries and include blown vessels, both colourless and weakly coloured samples, some objects with scratch decorations and some cobalt-blue fragments (Brill, 1995; Fig. S4).

2.2. Analytical methods

The compositional analysis of the glass samples was conducted at the Ernest-Babelon Centre of IRAMAT (Orléans, France). A VG UV-laser was used, generated by a Nd YAG pulsed beam and operating at 266 nm wavelength, 3–4 mJ power and 7 Hz repetition rate. Ablation time was set to 70 s:20 s for pre-ablation so that potential surface contaminations could be removed, and 50 s collection time. Pit ablation mode was used with spot sizes set to 100 μm or reduced down to 60 μm to avoid saturation of the detector by elements such as Mn. Blanks were run every 10 samples. An argon stream (1.15–1.35 l/min) carried the ablated material to the plasma torch of an Element XR mass spectrometer from Thermofisher Instruments (Gratuze, 2016). This system offers the advantage of being equipped with a three-stage detector: a dual mode (pulse-counting and analog modes) secondary electron multiplier with a linear dynamic range of over nine orders of magnitude, associated with a single Faraday collector, which increases the linear dynamic range by an additional three orders of magnitude. This feature allows the analyses of major, minor, and trace elements in a single run, independent of their concentrations and isotopic abundance. Measurements were made in peak jump acquisition mode, with four points per peak in the case of pulse-counting and analog detection modes, and ten points per peak when using Faraday detection. For most elements, the automatic detection mode was used; only sodium, silicon, aluminium and potassium were systematically measured with the Faraday detector. For silicon, the isotope ^{28}Si was measured and used as an internal standard. A total of 58 elements were thus recorded. With the chosen analytical parameters, the scan time required to measure the selected isotopes was about 2.5 s. Since most of the isobaric interferences encountered could be dealt with by working with non-interfered isotopes, all measurements were performed in low resolution mode. External calibration was performed against Standard Reference Materials from the National Institute of Standards and Technology (NIST SRM) 610, the Corning reference glasses B, C, and D, as well as an archaeological glass sample (APL1) for chlorine quantification. The signals were converted into quantitative compositional data following the procedures detailed by Gratuze (2016). Reference materials Corning A and NIST SRM612 were analysed at regular intervals as unknowns to determine the accuracy and precision of the analyses. For the major elements, the analysed values were within 5 % relative and for most trace elements within 10 % relative of the reference material. The coefficients of variation for all major elements were <5 %, for most minor and trace elements <5 % and always <10 %.

2.3. Multivariate statistical analysis

Based on the variables most useful for grouping the samples (Na_2O, MgO, Al_2O_3, SiO_2, P_2O_5, K_2O, CaO, Li, Ti, V, Cr, Rb, Sr, Y, Zr, La, Ce, and the ratio Cr/La) converted to log-ratios (Aitchison, 1999), we applied Minitab version 20.1.3 for Principal Components Analysis (PCA) and Cluster Analysis (CA) to a dataset of 154 of the Iranian plant-ash glasses (omitting six samples identified as outliers or Levantine), 40 samples from Samarra including 20 from Samarra group 1 and 20 from Samarra group 2 (Schibille et al., 2018), and 21 Sasanian samples from Veh Ardašīr (Mirti et al., 2008, 2009). The comparative data were selected because they appeared to be similar to the Iranian glasses based on prior PCA and CA of a larger dataset (not shown). For CA we applied the average method in Minitab, where the Euclidean distance between all variables is considered simultaneously. A similarity index of 97 % can be considered to represent analyses from the same or very closely related samples (Lankton et al., 2022), while values on the order of 80 % to 90 % indicate similar production technology and raw materials. Overall, the results of both PCA and CA (Figs. S5–S7) largely confirm our empirical grouping of the data.

3. Results

In the first publication on the composition of the glass from Nishapur, the assemblage was classified into colourless (water-white) and coloured (including naturally coloured) glass (Brill, 1995). This classification was maintained in most subsequent scholarly publications (Henderson et al., 2016; Phelps, 2017; Wypyski, 2015). Although there is some significance to this distinction, we initially present our new analytical data independently of context, typology (except for beads) or colour in order to reduce any possible bias and assess the compositional data on its own terms. It is important to emphasise that large amounts of additives necessarily distort the absolute concentrations of the base glass elements. Using element ratios to classify the samples mitigates this problem. That said, our present dataset contains few samples with high levels of colourants and/or opacifiers (Supplementary Table S1).

3.1. Compositional variability of the Iranian glass assemblages

The full raw data are given in the supplementary materials (Supplementary Table S1) separated by glass groups to which the individual samples were ultimately assigned. In addition, the averages and standard deviations of each group are also reported here to facilitate intergroup comparisons (Table 1). As anticipated, the analysed samples are all soda-lime-silica glass, of which all but four vessels have potassium and magnesium oxide in excess of 1.5 wt%, meaning they have been produced from soda-rich plant ash as the fluxing agent. When classifying plant ash glass, both the elements related to the fluxing agent and those associated with the silica source must be considered. A complicating factor is the possibility that the same plant ash can be combined with different silica sources and vice versa. This scenario has been observed,

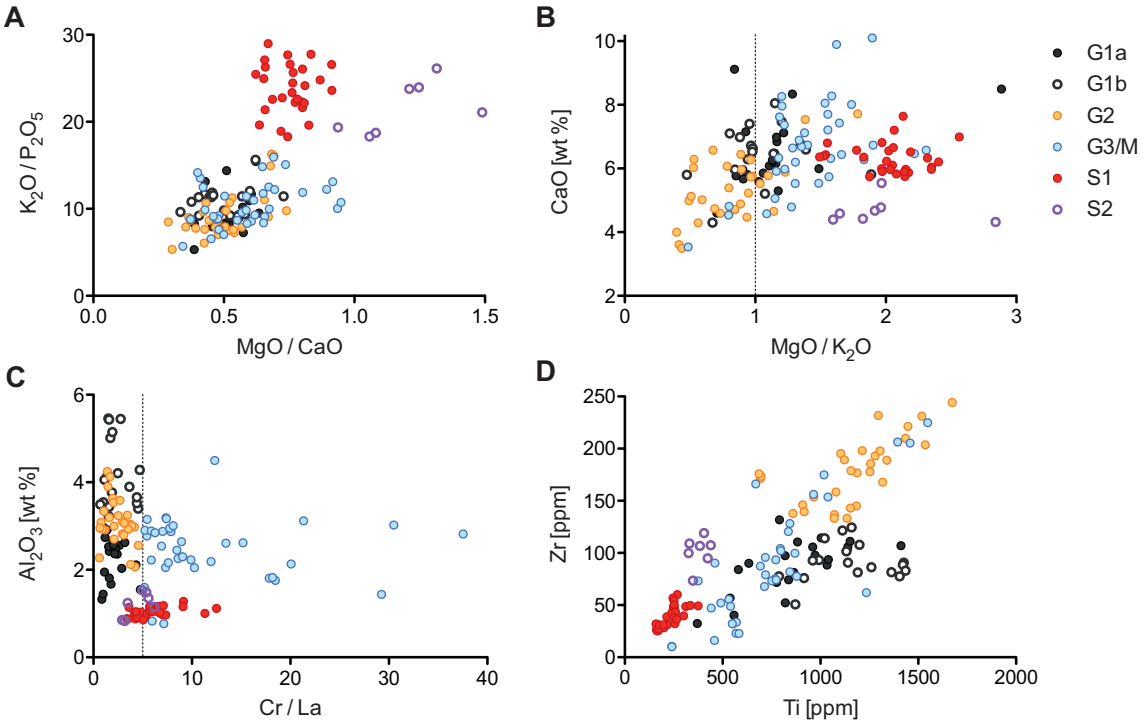

Fig. 3. Base glass characteristics of the main groups identified at the five Iranian sites. (A) MgO/CaO versus K_2O/P_2O_5 distinguish two main plant ash groups; (B) the ratios of MgO/K_2O allow further subdivisions in that group G2 tend to have less MgO relative to K_2O than most other groups while CaO is fairly constant across the different groups; (C) elevated Cr/La ratios single out silica group G3/M, while aluminium levels vary greatly across the different groups; (D) differences in the absolute concentrations and ratios of Zr and Ti confirm different base glass types.

for instance, in case of Sasanian glass from Veh Ardašīr (Ganio et al., 2013; Mirti et al., 2009, 2008).

Magnesium, potassium, calcium, phosphorus and lithium are elements diagnostic of the plant ash component and/or ashing processes (Schibille, 2022). Among the studied Iranian samples, two macro-groups can thus be defined: a main plant ash type with moderate magnesium, potassium, phosphorus and calcium concentrations that represents about 75 % of all samples (Groups G1, G2, G3/M), and the remaining 25 % (Groups S1, S2) that has notably higher magnesium (MgO > 4 %), but considerably lower phosphorus (P_2O_5 < 0.15 wt%) and to a lesser extent potash contents. These differences are reflected in higher ratios of MgO/CaO, MgO/K_2O and K_2O/P_2O_5: MgO/K_2O of ~2 compared to ~1; MgO/CaO of ~1 compared to ~0.5; K_2O/P_2O_5 ~ 20 compared to ~10 (Fig. 3A, B; Table 1). Some further subdivisions can be made. For example, what we call silica group G2 has on average lower magnesium relative to potassium (MgO/K_2O < 1) and lower calcium contents (Fig. 3B; Table 1). Similarly, a subset of 7 samples from the high MgO low P_2O_5 group have slightly higher Na_2O and K_2O and lower CaO concentrations. CaO concentrations in all other groups remain fairly constant, averaging between 6 wt% and 7 wt%. Hence, at least two, maybe three or four different plant ash components underlie the glasses in this study. It must be said that plant ash is a highly variable constituent and some variations may be due to differences in the plant parts or ash preparations or the season in which the plants were collected (Barkoudah and Henderson, 2006). In short, we cannot derive any firm conclusions about the origin of these glasses from differences in the plant ash elements alone.

In addition to the consideration of plant-ash related elements, it is important to take into account minor and trace elements derived from the silica source in order to distinguish different primary production events and possibly production regions. Aluminium, chromium and zirconium and particularly the ratios of Cr/La and Zr/Ti are effective discriminants to separate the majority of samples (Fig. 3C, D). A quarter of the assemblage (n = 35) that was shown to have a very distinct plant ash signature has very low mineral impurities such as aluminium, titanium, chromium and zirconium, indicative of the use of a clean, quartz-rich silica source similar to the glass found at Samarra (Schibille et al., 2018). The group separates into two sub-types. 28 samples (group S1) have exceptionally low aluminium (Al_2O_3 ~ 1 wt%), titanium (TiO_2 ~ 0.04 wt%) and iron (Fe_2O_3 ~ 0.29 wt%) and moderate zirconium values (Zr ~ 40 ppm), while the 7 samples of group S2 with higher alkali levels also show slightly higher aluminium (Al_2O_3 ~ 1.2 wt%) and particularly higher titanium (TiO_2 ~ 0.08 wt%), zirconium (Zr ~ 100 ppm) and cerium concentrations (Table 1). Most colourless glasses that were analysed belong to these two closely related groups.

The other compositional groups are not as easily defined and require a reiterative process of comparing elements and their ratios. One silica group G3/M is characterised by elevated Cr/La ratios > 5 (Fig. 3C). This threshold was recently proposed to distinguish Mesopotamian glass from both Levantine and Central Asian vitreous materials, albeit with concessions when dealing with very clean material such as the glass from Samarra (corresponding to S1 and S2 in the present study), which lie either side of the threshold (Schibille, 2022; Schibille et al., 2018). Group G3/M is highly variable in terms of its macroscopic features (Fig. S3) as well as its mineral contaminants some of which range over more than one order of magnitude such as zirconium (10 ppm < Zr < 225 ppm). It can therefore be assumed that this group represents several independent production events, all of which are characterised by elevated chromium positively correlated with iron and vanadium (Fig. 5B), and higher magnesium relative to both potassium and calcium compared to silica groups G1 and G2 (Fig. 3A, B; Table 1). We refrain from further subdivisions here, as the relatively small number of samples would make it difficult to draw valid conclusions.

The two silica groups G1 and G2 overlap in many respects. Neither has conspicuous chromium signatures (Cr/La < 5), while both contain on average more silica-related impurities such as aluminium, titanium, zirconium and cerium (Fig. 3C, D; Table 1). Group G2 differs from G1 mainly in its higher zirconium concentrations with a clear positive

Table 1
Average compositions and standard deviations of glass groups identified among early Islamic Iranian assemblages.

	wt%										ppm											MgO/CaO	MgO/K_2O	K_2O/P_2O_5	Cr/La
	Na_2O	MgO	Al_2O_3	SiO_2	P_2O_5	Cl	K_2O	CaO	TiO_2	MnO	Fe_2O_3	Li	Cr	Rb	Sr	Zr	La	Ce	Th					
G1a (n = 21)	16.0	3.38	2.27	65.0	0.33	0.73	3.11	6.48	0.15	0.78	1.14	20.2	22.8	14.9	572	88.1	11.5	21.5	2.43		0.52	1.09	9.30	1.99
Stdev	1.6	0.64	0.47	1.5	0.07	0.12	0.65	1.08	0.04	0.56	0.74	13.0	9.9	3.3	133	25.1	3.0	5.8	0.46					
G1b (n = 18)	16.3	3.18	4.18	62.2	0.30	0.82	3.14	6.48	0.19	0.27	1.57	16.7	25.5	22.3	520	91.1	11.2	20.7	3.08		0.49	1.01	10.6	2.27
Stdev	1.0	0.55	0.76	2.7	0.06	0.17	0.44	0.84	0.03	0.25	0.55	10.6	11.8	4.2	115	17.4	1.8	3.0	0.39					
G2 (n = 30)	15.6	2.64	3.09	66.0	0.38	0.67	3.33	5.36	0.20	1.09	1.17	16.1	28.4	20.0	428	180	12.9	19.6	2.79		0.49	0.79	8.68	2.20
Stdev	1.3	0.62	0.49	2.0	0.10	0.20	0.60	0.99	0.04	0.80	0.47	6.7	10.3	5.5	123	33	4.1	3.9	0.55					
G3/M (n = 37)	15.5	3.86	2.42	65.2	0.28	0.77	2.79	6.80	0.12	0.71	1.17	19.7	72.3	15.9	452	88.1	6.95	13.1	1.91		0.57	1.39	10.0	10.4
Stdev	2.0	0.83	0.73	2.9	0.07	0.20	0.56	1.65	0.05	0.63	0.60	18.1	39.3	6.2	128	55.8	2.78	5.1	0.75					
S1 (n = 28)	12.2	4.75	1.02	71.8	0.10	0.62	2.38	6.32	0.04	0.36	0.29	21.1	31.2	13.2	356	39.4	3.17	6.10	0.95		0.75	2.00	23.7	9.83
Stdev	1.0	0.36	0.11	1.2	0.01	0.08	0.27	0.46	0.01	0.11	0.07	3.6	61.4	1.1	46	10.2	0.28	0.86	0.10					
S2 (n = 7)	14.9	5.53	1.21	68.7	0.13	0.58	2.87	4.67	0.06	0.80	0.35	23.8	28.3	12.0	423	102	6.28	11.8	1.53		1.18	1.92	21.6	4.50
Stdev	0.5	0.58	0.26	0.8	0.01	0.07	0.42	0.39	0.01	0.59	0.13	4.0	7.0	2.5	11	13	0.28	0.4	0.08					

correlation with titanium. G2 has also one of the lowest ratios of magnesium to potassium and the highest phosphorus levels. It is more narrowly clustered than groups G1 and G3, and it appears to represent a relatively homogeneous glass group. Of the 30 samples assigned to group G2, 26 fragments, including five pieces of working debris, are from Gorgan close to the Caspian Sea, somewhat off the beaten track of the main Silk Road system. This potentially indicates a local or regional production. Many of the samples contain copper and/or lead above the natural background levels of the raw materials (>100 ppm), suggesting either the accidental (i.e. recycling) or deliberate incorporation of colourants or coloured glass cullet. As a result, most fragments are more or less strongly coloured. Nishapur sample NIS 3081, for instance, has an emerald green colour due to a high content of copper (CuO ~ 3.3 wt%).

Silica group G1 shows a wide range of accessory minerals. The group as a whole does not exhibit any clear features and further classification is warranted. Using aluminium concentrations, group G1 can be tentatively separated into a low (Al_2O_3 < 3 wt%) and a high aluminium group (Al_2O_3 > 3 wt%). The high aluminium group also tends to have higher rubidium contents (Table 1). While the two sub-types do not differ much in the absolute concentrations of titanium, zirconium or thorium (Table 1), both titanium and thorium tend to be somewhat higher relative to zirconium in the high aluminium group (G1b; Fig. 3D). Many of the samples attributed to G1b also have lower magnesium relative to potassium (MgO/K_2O < 1). According to the current state of affairs, these compositional differences probably signal different productions and by extension different places of manufacture (Brill, 1995; Henderson et al., 2016; Phelps, 2018; Schibille, 2022). Cluster Analysis (CA) provides strong support for our empirical groupings including the subdivision of Groups G1a and G1b, with minor differences in group affiliation of < 5 % of the samples (Figs. S6–S7).

3.2. Miscellaneous & beads

Three of the four natron-type glasses are scratch decorated vessels from Nishapur, of which two are blue and the other one is near colourless (Supplementary Table S1). They have fairly low Al_2O_3 and high CaO concentrations but low Sr/CaO ratios, elevated titanium and zirconium and thus correspond to Egypt 2 glass (Gratuze, 1988; Schibille et al., 2019). Egypt 2 was produced from the second half of the eighth until the end of the ninth century CE at an as yet unknown location in Egypt (Schibille et al., 2019). The blue fragments are coloured by a combination of cobalt and copper with an excess of zinc, elevated iron; one sample also shows high arsenic and antimony contents. This type of colourant is associated with Islamic glass production in the Near East from the eighth century on (Gratuze et al., 2018). One bluish vessel from Qom has all the characteristics of Roman manganese decoloured glass with moderate Al_2O_3, CaO and low Ti and Zr contents (Freestone, 2020; Schibille, 2022).

Two of the plant ash glasses that were analysed (Qom 05, NIS 5303) are consistent with early Islamic plant ash glass produced in the Levantine area (Phelps, 2018; Schibille, 2022). Compared to the main Mesopotamian and Iranian glasses described above, they have lower magnesium relative to both potassium and calcium contents, somewhat higher phosphorus and low lithium, moderate aluminium as well as low titanium, chromium and zirconium (Supplementary Table S1). Five vessel fragments (Supplementary Table S1) have somewhat unusual characteristics that impede a clear classification.

Of the 15 bead fragments, four beads (NIS BC 14, NIS BC 30, NIS 5335, HAM 5346) have high MgO/K_2O, K_2O/P_2O_5 and Cr/La ratios, reflective of a Mesopotamian origin. NIS BC 14 is a pale yellow nearly colourless bead that appears to have been blown. Its composition is similar to Samarra group 2. Sample NIS 5335 is a cobalt-blue wound bead with blue and white stratified eyes that are marvered flush to the bead surface (Fig. 2). The blue body and the white eye layer are very similar in composition, indicating that the same base glass was coloured either blue by cobalt or white by a combination of tin and lead

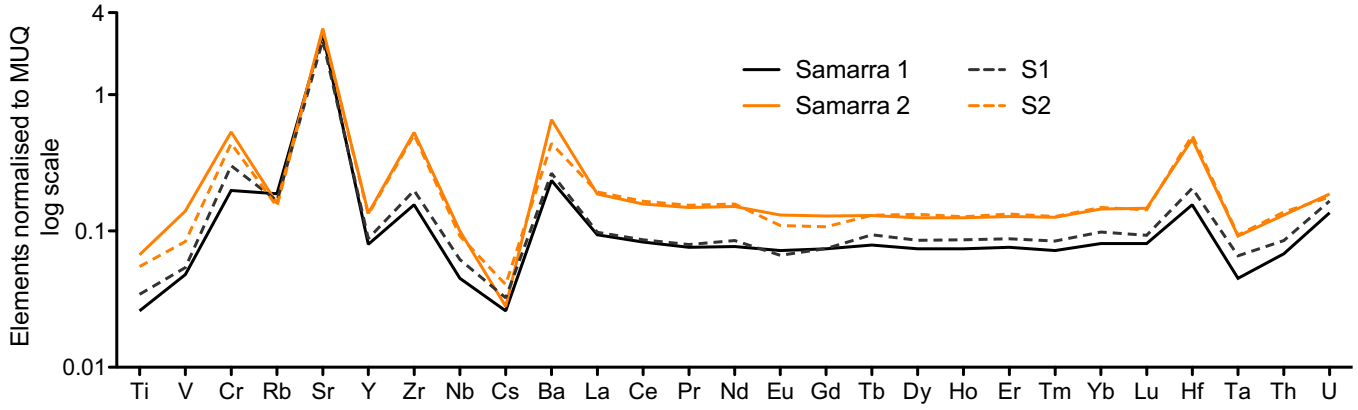

Fig. 4. Trace element profile of the Samarra Type S1 and Type S2 samples compared to the data from Samarra. Group average trace elements were normalised to their relative abundance in the upper continental crust (MUQ; Kamber et al., 2005).
Data for Samarra from Schibille et al. (2018).

(Supplementary Table S1). All three phases are similar to Mesopotamian group G3/M, however, the blue eye decoration is different from the blue body, suggesting that glass from multiple sources were worked in the same beadmaking workshop. The individual parts of the mosaic eye bead found at Hamadan (HAM 5346) also show differences in composition. The bead was made by winding white glass around a mandrel, trapping air bubbles in the process (Fig. 2). Small chips of mosaic cane were then pressed into the surface of the white glass and smoothed into place. With the exception of the black glass, all other bead parts show typical features of Mesopotamian glass. The black glass is coloured by a combination of iron and manganese, the red glass owes its colour to copper (Supplementary Table S1). Both white glasses have tin and lead as the main colourant and opacifier, although in different concentrations. This may indicate that the mosaic cane was prepared elsewhere or at a different time than the final bead.

Among the Nishapur beads, the fragments NIS BC 23 and NIS BC 29 most likely belong to the same dark green/black bead (Supplementary Table S1). The glass is heavily weathered and unlike the other early Islamic samples. The two opaque red glass bead fragments NIS BC 15 and NIS BC 24 are also similar but different from the other samples. They have unusually high antimony and in case of sample NIS BC 24 also very high arsenic concentrations. These beads may be the result of mixing and recycling and/or later intrusions. The black wound bead NIS BC 02 (Fe_2O_3 = 4.35 wt%) is compositionally linked to the Iranian group G2 rather than Mesopotamian glass. Finally, a number of beads may represent older materials. Three beads (NIS BC 19, 22, 25) were made from Roman natron-type glass (Supplementary Table S1). A bead from Rayy (RAY BC 02) with exceptionally high chromium (217 ppm) was made by folding a glass pad around an iron mandrel, leaving a visible longitudinal seam (Fig. 2). This technique was more common during the Achaemenid period.

4. Discussion

4.1. Comparison with regional glass production groups

4.1.1. Brill's colourless glass – Nishapur 1a/Samarra 1

As mentioned above, the truly colourless glass from Nishapur, plus some samples from Gorgan and Qom (group S1, Fig. S4) is tightly clustered due to the use of a clean, quartz-rich network former with low mineral impurities. It corresponds to what one of the present authors previously called Nishapur 1a (Schibille, 2022), similar to Wypyski's Nishapur A (Brill, 1995; Wypyski, 2015). This glass closely resembles Samarra 1 (Fig. 4), a ninth-century glass used, among other things, for

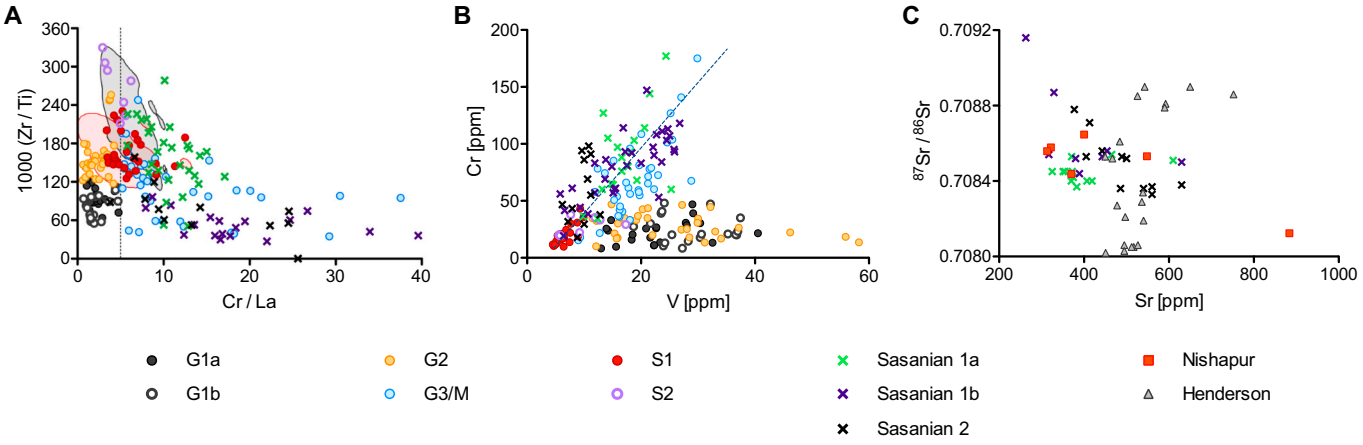

Fig. 5. Data of Iranian groups compared to Sasanian glass from Veh Ardašīr and Samarra 1 and Samarra 2. (A) Cr/La and Zr/Ti ratios showcase the similarities between groups S1 and S2 with Samarra 1 and Samarra 2 given as 95 % kernel density contours (Samarra 1 in red, Samarra 2 in grey) and between silica group G3/M and Sasanian 1 from Veh Ardašīr; (B) chromium is positively correlated in group G3/M similar to Mesopotamian glass from Samarra and Veh Ardašīr; (C) strontium isotope signatures confirm that the plant ash underlying the Nishapur samples and that used in Sasanian glass from Veh Ardašīr are geologically related. (For interpretation of the references to colour in this figure legend, the reader is referred to the web version of this article.)
Data sources: Ganio et al. (2013), Mirti et al. (2009), and Mirti et al. (2008).

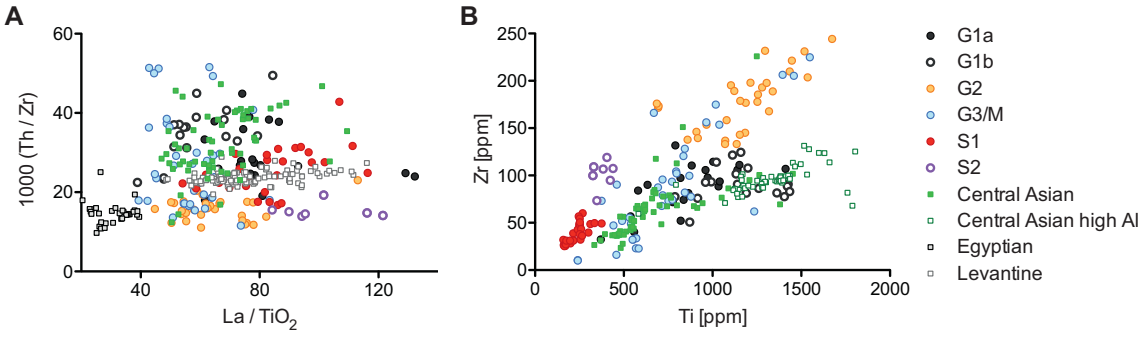

Fig. 6. Data of Iranian groups compared to Central Asian glass from Merv. (A) ratios of La/TiO_2 and Th/Zr exclude Egyptian, Levantine and Mesopotamian glasses as potential sources of groups G1 and G2, while group G1b seems consistent with Central Asian glass types; (B) different slopes of Ti to Zr regression lines suggests different base glass types for groups G1, G2 and Samarra-type glasses.
Data sources: Meek et al., Phelps (2017), Schibille et al. (2019), and Schibille et al. (2018).

architectural decorations at Samarra and probably manufactured in the vicinity of al-Mu'tasim's city on the banks of the river Tigris (Schibille et al., 2018). The Iranian samples with a Samarra-type S1 signature have on average slightly higher trace and rare earth elements than group 1 from Samarra itself, but this may be a sampling effect or the result of cut-offs that were introduced to separate the subgroups. The small group of 7 samples (group S2) with higher accessory elements is consistent with Samarra 2. Samarra 2 makes up the bulk of the vitreous material at Samarra and underlies strongly coloured architectural glasses as well as glass vessels with a faint bluish or greenish tinge (Schibille et al., 2018). Although it is impossible to prove the identity of groups S1 and S2 from the Iranian sites with those from Samarra, the compositional features of the plant ash component (very high MgO, low P_2O_5) and the silica source (very low accessory minerals, but relatively high Cr/La) strongly favour a Mesopotamian origin of these glasses. Compositional evidence suggests that the colourless Samarra 1 glass type was traded widely throughout the Islamic world, to Egypt (Brill, 1999), the Levant (Phelps, 2018), al-Raqqa (Henderson et al., 2016), and all the way to Japan (Abe et al., 2018). The frequency distribution of the joint groups S1 and S2 between the different sites analysed in this study favours a provenance in the Tigris valley thus lending support to a production site in or near Samarra (Schibille et al., 2018; Fig. 7).

4.1.2. *Group G3/Mesopotamian*

A Mesopotamian origin can also be suggested for group G3/M, due to the elevated Cr/La and MgO/K_2O ratios, which are probably linked to the geochemistry of the Euphrates and Tigris river valleys (Henderson et al., 2016; Shortland et al., 2007). Chromite-bearing sands underlie, for example, the glass from Samarra, Veh Ardašīr, Ctesiphon and Siraf (Henderson et al., 2016; Mirti et al., 2009, 2008, Schibille, 2022;

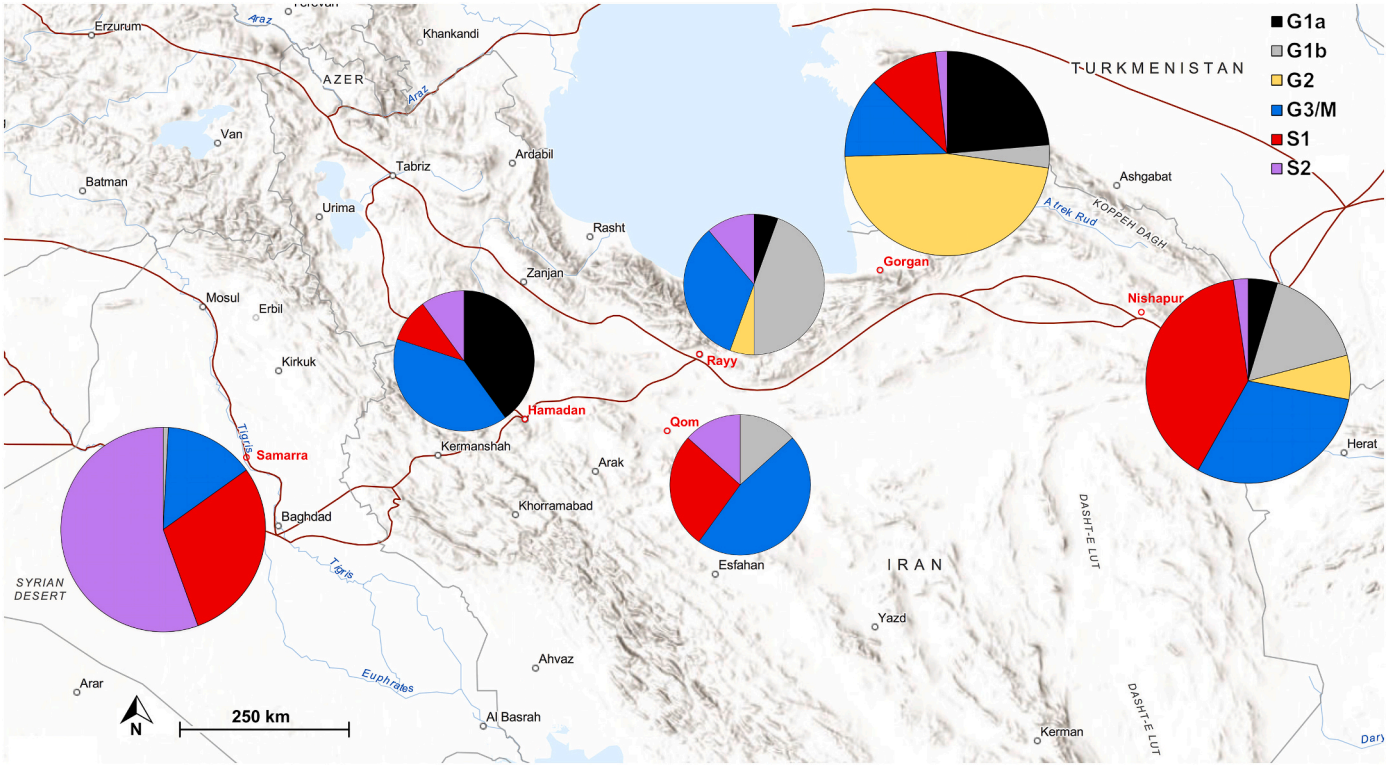

Fig. 7. Glass group distribution in Iran and Samarra (Iraq). The frequency distribution suggests that groups S1 and S2 as well as G3/M are Mesopotamian, while G1 and G2 are more likely from further east (Iran/Central Asia). Created using worldmap from ArcGIS hosted by Esri, USGS (https://worldmap.maps.arcgis.com/apps/mapviewer/index.html). Layers used by StoryMaps.

Schibille et al., 2018; Swan et al., 2017). Group G3/M exhibits clear similarities with Sasanian glasses from Veh Ardašīr (Figs. S5–S7), more specifically with Sasanian 1 in terms of both the silica source as well as the plant ash component. In both cases, vanadium and chromium are positively correlated, while Zr/Ti ratios are variable (Fig. 5A, B). Aluminium levels are moderate and magnesium levels are comparatively high and typically higher than the potassium concentrations (Fig. 3B). The strontium isotope data that are available for some of the glass samples from Nishapur (Brill and Stapleton, 2012) also coincide with the strontium isotopes of the glass from Veh Ardašīr (Ganio et al., 2013), indicating the use of ash from plants grown in geologically related environments (Fig. 5C). In the absence of evidence to the contrary, a Mesopotamian production of these glasses therefore seems likely.

PCA and CA support the group assignments based on elements and ratios, and add nuance to the results, opening the possibility to compare broadly grouped samples with those from specific source areas. Iranian group G3/M is a good example: while a few of the G3/M samples are similar to Sasanian groups 1b and 2, most of the G3/M glasses are more like Sasanian group 1a, found at Veh Ardašīr in third- to seventh-century contexts and produced, possibly nearby, using plant ash and a silica source relatively high in trace elements including Zr and REEs. The similarity between Iranian G3/M and Sasanian 1a (Figs. S5–S7) demonstrates the persistence of Mesopotamian glassmaking technologies and use of raw materials.

4.1.3. Groups G1 & G2

Silica groups G1 and G2 cannot be positively attributed to any established primary production zone, but Egypt (Schibille et al., 2019), the Levant (Phelps, 2017) and Mesopotamia (Schibille et al., 2018) can be excluded as potential sources (Fig. 6). The zirconium and titanium contents of groups G1a and G1b appear to lie approximately on the same regression line as Central Asian glass from Merv (Fig. 5; Meek et al.) that deviates clearly from that of Samarra 1 and Samarra 2 as well as of groups G 3/M and G2. Whether the similarities in composition of group G1 and central Asian glass indicate that they have originated from the same production area cannot be decided from the analytical data, due to the lack of sufficient comparative material and archaeological evidence. Statistical cluster analysis separates the G1 groups from the Central Asian samples from Merv, which may point to separate production zones (data not shown). Based on circumstantial evidence and current knowledge, it can be surmised that all these glass types were produced east of the Zagros Mountain range on the Iranian plateau and/or Central Asia (Henderson et al., 2016; Schibille, 2022).

Group G2 seems to be the odd one out, as no clear compositional match was found. The glasses of this group are in many respects related to the glasses of group G1, but for their high contents of zirconium. By implication, they probably came from an Iranian/Central Asian glassmaking centre. Based on the group structure and the frequency distribution of the glass, we can venture the hypothesis that this glass may have been manufactured in the area around Gorgan itself. Glass furnaces were found there and our dataset includes some glass working debris that strongly supports the presence of local vessel production, if not production of the raw glass itself. Many of the G2 samples have a pronounced greenish colour due to elevated iron and/or copper concentrations and appear to have been used for the manufacture of domestic ware rather than destined for long-distance trade (Supplementary Table S1; Fig. S2).

4.2. Mapping compositional groups

Mapping glass groups found at individual sites reveals geographical distribution patterns that can indicate likely productions zones, even though the extent of movement of particular glass types may vary. More than 70 % of the glass assemblage found at Nishapur is of the Samarra type or silica group G3/M, which presumably travelled over a distance of about 1600 km to reach its destination. The remaining 30 % consist of the Iranian types G1 and G2, which were probably imported from the surrounding regions. Whether or not there was any local glass production at Nishapur as has been assumed (Brill, 1995; Collinet, 2015; Henderson et al., 2016; Phelps, 2018) cannot be conclusively decided at present, but seems increasingly unlikely. The two glass types with low impurities (S1 and S2) previously attributed to local glassmaking have been shown to be Mesopotamian, because they are practically indistinguishable from Samarra 1 and Samarra 2. Both types predominate at Samarra itself where they were used for high-end architectural decorations (Fig. 7; Schibille et al., 2018). The supposedly Iranian glass groups are in the minority at Nishapur and occur in greater relative abundance at the other sites that have been investigated. All this argues against local glass production at Nishapur.

The group structure of the assemblage from Gorgan is in complete contrast to this. Here, <30 % of the samples are compatible with Mesopotamian imports, while group G2 represents the largest fraction of the assemblage ($n = 26$), which may be a regionally or perhaps even locally produced glass. Five pieces of glass working debris belong to this group as do some coloured samples, especially some Co/Cu blue fragments, one unguentarium with red trails marvered into a black-appearing body (Gor BC 18), an amber coloured vessel (Gor BC 25) as well as purple and turquoise trail decorations on a bottle neck (Gor BC 02; Fig. S1; Supplementary Table S1). The only other places where G2-type glass was found are Rayy and Nishapur. At both sites, the G2 samples are strongly coloured. At Rayy two dark blue samples were recovered, and at Nishapur, two green and two blue fragments match the G2 composition, of which the copper-green sample (NIS 3081) has wheel cut decorations (Fig. S2).

Most of the other copper (emerald) green samples among the analysed fragments belong to group G1, which is proportionally the most abundant group at Rayy (Teheran). Here, the two putative Iranian glass types G1 and G2 predominate, but Mesopotamian Samarra 2 and G3/M are also represented (Fig. 7), the latter showing clear signs of recycling in the form of high levels of copper and lead. Further south and southwest, at Qom and Hamadan, Mesopotamian glass types (S1, S2, G3/M) increase proportionally, while recycling indicators seem to be a tad weaker, perhaps due to the relative proximity of the two provinces to Baghdad and the Tigris valley. Another interesting observation is that groups G1a and G3/M are represented in equal proportions in Hamadan, whereas G1a is absent from the assemblage at Qom. Due to the small number of samples, not much can presently be gleaned from this discrepancy. One difference between the two sites is that Hamadan was located on two major thoroughfares, the Great Khorasan route connecting Mesopotamia and the Iranian Plateau, and the Royal Road leading north, whereas Qom is bordered by a mountain range to the north-east and west. In any case, there seems to be a tendency that the more northern parts of the Iranian Plateau show a higher frequency of the G1a glass. We may conclude from this that the source of the G1a type glass may be found in northern Iran and that there was some movement along the east-west axis of the Silk Roads, since G1a glass is present in all the regions except Qom. The distribution of silica group G1b has a more (south-) eastern trend, especially if one takes into account that three of the samples from Rayy have a very similar composition, which suggest that they may be from the same batch/object (Supplementary Table S1). This could mean that the primary production of this glass type lies further east, thereby confirming a gradient of aluminium concentrations from east to west (Phelps, 2018). High aluminium concentrations characterise a glass sub-category at Merv (Turkmenistan), which may be indicative of a Central Asian provenance (Meek et al.).

The cobalt concentrations in the blue samples (Co > 100 ppm) also vary regionally. The highest cobalt contents are found among the glasses of the Mesopotamian G3/M group and in one sample from Gorgan (BC GUR 24) with a G1b base glass composition. Several cobalt ore deposits are known in central Iran, most famously the cobalt mine at Qamsar close to Kashan (Fig. 1), which yielded mainly cobaltite (CoAsS) and

erythrite ($Co_3(AsO_4)_2{\cdot}8(H_2O)$) (Matin and Pollard, 2017, 2015). The cobalt extracted and processed from these mines is thus associated with elevated As and Fe but it does not contain any significant quantities of Ni, Cu or Zn (Matin and Pollard, 2017). It has recently been shown that the Qamsar mine was not yet exploited in the early Islamic period (Matin and Pollard, 2017). In this context it is interesting to note that of the 24 cobalt-blue plant ash glass samples analysed in this study only three have elevated arsenic, and all three may be dated to the eleventh or twelfth century CE (Supplementary Table S1). The others have much higher levels of copper, zinc and nickel, and the compositional fingerprint of the cobalt ore is thus not easily visible. From the mapping of the cobalt blue samples in relation to the base glass groups identified in this study we may nonetheless infer a source of cobalt in the central/western area of the Iranian Plateau. It needs to be emphasised, however, that copper, zinc and nickel may have been introduced separately to the glass batch and that cobalt has always been widely traded throughout the Islamic world and beyond (Colomban et al., 2021).

5. Conclusions

Our compositional characterisation of early Islamic glass assemblages from Iran refines previous models of regional glass production zones by focusing on the Iranian plateau. The profile of glasses from the Iranian sites contrasts greatly with Mesopotamian glass groups that have very distinct trace element signatures particularly as regards elevated Cr/La ratios, but often also relatively high MgO/CaO and K_2O/P_2O_5 ratios. By mapping the glass groups within different regional assemblages, it is possible to outline large-scale patterns in the circulation of vitreous materials, regional connections, and to hypothesise about where the different glass groups might be coming from. The available data show the region around Samarra as the likely location of primary production of glass during the early Islamic period, given that the glass finds are overwhelmingly of the Samarra 1 and Samarra 2 type. Primary production of glass may also have existed to the east of the Zagros Mountains, possibly at Gorgan and other sites not yet identified. Nonetheless, there is no conclusive evidence for primary glassmaking at Nishapur. This geographical and chronological picture is certain to evolve as more data become available.

It is important to remember that a high concentration of a specific glass type in one place does not necessarily have to be directly linked to local primary production; rather, it can provide information about where certain glasses were actually used that in turn may reveal something about the social and economic contexts of these sites. The contrast between Nishapur and Gorgan is a case in point. The glass assemblage at Nishapur clearly reflects the city's importance as a trading centre, where much of the vitreous material was imported. Gorgan, on the other hand, appears to have been more isolated, and glass with a local or regional character was used to produce glassware of daily use, which was not traded widely.

Supplementary data to this article can be found online at https://doi.org/10.1016/j.chemer.2022.125903.

Funding

This project has received funding from the European Research Council under the European Union's Horizon 2020 - Research and Innovation Framework Programme (GlassRoutes, grant agreement No. 647315 to NS). The funding organisation had no influence in the study design, data collection and analysis, decision to publish, or preparation of the manuscript.

Data statement

All data generated within this study are made available in the published article and its supplementary material.

CRediT authorship contribution statement

Nadine Schibille: conceptualization, formal analysis, investigation, writing original draft, visualization, funding acquisition, revisions;
James Lankton: conceptualization, formal analysis, investigation, writing original draft, visualization, revisions;
Bernard Gratuze: conceptualization, formal analysis, investigation, resources, revisions.

Declaration of competing interest

The authors declare that they have no known competing financial interests or personal relationships that could have appeared to influence the work reported in this paper.

Acknowledgments

We would like to thank Katherine Larson, Stephen Koob and Karol Wight at the Corning Museum of Glass for giving access and allowing us to analyse the glass from the Brill Scientific Research Collection, and to Robert Brill for his strong encouragement in the early stages of this study.

References

Abe, Y., Shikaku, R., Nakai, I., 2018. Ancient glassware travelled the Silk Road: Nondestructive X-ray fluorescence analysis of tiny glass fragments believed to be sampled from glassware excavated from Niizawa Senzuka Tumulus No. 126, Japan. J. Archaeol. Sci. Rep. 17, 212–219.
Aitchison, J., 1999. Logratios and natural laws in compositional data analysis. Math. Geol. 31, 563–580.
Barkoudah, Y., Henderson, J., 2006. Plant ashes from Syria and the manufacture of ancient glass: ethnographic and scientific aspects. J. Glass Stud. 48, 297–321.
Bosworth, C.E., 2012. GORGĀN vi. History from the Rise of Islam to the Beginning of the Safavid Period. In: Encyclopædia Iranica, XI/2, pp. 153–154 (accessed on 26 April 2022). http://www.iranicaonline.org/articles/gorgan-vi.
Bosworth, C.E., Blair, S., 2012. ASTARĀBĀD. In: Encyclopædia Iranica, II/8, pp. 838–840 (accessed on 26 April 2022). http://www.iranicaonline.org/articles/astarabad.
Brill, R.H., 1995. Appendix 3: Chemical analyses of some glass fragments from Nishapur in the Corning Museum of Art. In: Kröger, J. (Ed.), Nishapur: Glass of the Early Islamic Period. Metropolitan Museum of Art, New York, pp. 211–233.
Brill, R.H., 1999. Chemical Analyses of Early Glasses. The Corning Museum of Glass, Corning, New York.
Brill, R.H., Stapleton, C.P., 2012. Chemical Analyses of Early Glasses, Volume 3. Corning Museum of Glass, Corning, New York.
Bulliet, R.W., 2009. Cotton, Climate, and Camels in Early Islamic Iran: A Moment in World History. Columbia University Press, New York.
Bulliet, R.W., 2018. Why Nishapur? Euras. Stud. 16, 100–123.
Collinet, A., 2015. Nouvelles recherches sur la céramique de Nishapur: la prospection du shahrestan. In: Rante, R. (Ed.), Greater Khorasan: History, Geography, Archaeology and Material Culture. De Gruyter, Berlin/Munich/Boston, pp. 125–140.
Colomban, P., Kırmızı, B., Simsek Franci, G., 2021. Cobalt and associated impurities in blue (and green) glass, glaze and enamel: relationships between raw materials, processing, composition, phases and international trade. Minerals 11, 633.
De Juan Ares, J., Cáceres Gutiérrez, Y., Moreno Almenara, M., Schibille, N., 2021. Composition and origins of decorated glass from Umayyad Cordoba (Spain). Heritage Sci. 9.
Drechsler, A., 2009. Qom I. History to the Safavid Period. In: Encyclopædia Iranica, online edition (accessed on 26 April 2022). https://www.iranicaonline.org/articles/qom-i-history-safavid-period.
Freestone, I.C., 2020. Apollonia glass and its markets: an analytical perspective. In: Tal, O. (Ed.), Apollonia-Arsuf Final Report of the Excavations, Volume II: Excavations outside the Medieval Town Walls. University Park, Pennsylvania, Eisenbrauns, pp. 341–348.
Frye, R.N., 2012. Hamaḏhān. In: Bearman, P., Bianquis, T., Bosworth, C.E., Donzel, E.v., Heinrichs, W.P. (Eds.), Encyclopaedia of Islam, Second edition. Brill, Leiden. https://doi.org/10.1163/1573-3912_islam_SIM_2653.
Ganio, M., Gulmini, M., Latruwe, K., Vanhaecke, F., Degryse, P., 2013. Sasanian glass from Veh Ardašīr investigated by strontium and neodymium isotopic analysis. J. Archaeol. Sci. 40, 4264–4270.
Gratuze, B., 1988. In: Analyse non destructive des objets en verre, par des methodes nucleaires : application a l'etude des estampilles et poids monetaires islamiques. PhD thesis. Université Orléans.
Gratuze, B., 2016. Glass characterization using laser ablation-inductively coupled plasma-mass spectrometry methods. In: Dussubieux, L., Golitko, M., Gratuze, B. (Eds.), Recent Advances in Laser Ablation ICP-MS for Archaeology, Series: Natural Science in Archaeology. Springer, Berlin, Heidelberg, pp. 179–196.

Gratuze, B., Pactat, I., Schibille, N., 2018. Changes in the signature of cobalt colorants in late antique and early islamic glass production. Minerals 8, 225.
Hauser, W., Wilkinson, C.K., 1942. The museum's excavations at Nishapur. Bulletin of the Metropolitan Museum of Art 37, 83–119.
Henderson, J., Chenery, S., Faber, E., Kröger, J., 2016. The use of electron probe microanalysis and laser ablation-inductively coupled plasma-mass spectrometry for the investigation of 8th–14th century plant ash glasses from the Middle East. Microchem. J. 128, 134–152.
Holakooei, P., de Lapérouse, J.-F., Rugiadi, M., Carò, F., 2018. Early Islamic pigments at Nishapur, North-Eastern Iran: studies on the painted fragments preserved at The Metropolitan Museum of Art. Archaeol. Anthropol. Sci. 10, 175–195.
Kamber, B.S., Greig, A., Collerson, K.D., 2005. A new estimate for the composition of weathered young upper continental crust from alluvial sediments, Queensland, Australia. Geochim. Cosmochim. Acta 69, 1041–1058.
Kiani, M.Y., 1984. The Islamic City of Gurgan. Archäologische Mitteilungen aus Iran: Ergänzungsband. Deutsches Archäologisches Institut. Abteilung Teheran, Berlin.
Kröger, J., 1995. Nishapur: Glass of the Early Islamic Period. Metropolitan Museum of Art, New York.
Lankton, J.W., Pulak, C., Gratuze, B., 2022. Glass ingots from the Uluburun shipwreck: glass by the batch in the Late Bronze Age. J. Archaeol. Sci. Rep. 42, 103354.
Larson, K.A., 2021. Building a Collection: Ray Winfield Smith and the Corning Museum of Glass. In: Annales du 21e Congrès de l'AIHV (Istanbul, 3–7 September 2018), pp. 657–668.
Matin, M., Pollard, A., 2017. From ore to pigment: A description of the minerals and an experimental study of cobalt ore processing from the Kāshān Mine, Iran. Archaeometry 59, 731–746.
Matin, M., Pollard, M., 2015. Historical accounts of cobalt ore processing from the Kashan mine, Iran. Iran - J. of the British Institute of Persian Studies 53, 171–183.
Meek, A., Schibille, N., Simpson, S.J., 2021. Central Asian glass at the crossroads of the Silk Route: A ninth-century assemblage from Merv, Turkmenistan.
Mirti, P., Pace, M., Malandrino, M., Negro Ponzi, M., 2009. Sasanian glass from Veh Ardaŝīr: new evidences by ICP-MS analysis. J. Archaeol. Sci. 36, 1061–1069.
Mirti, P., Pace, M., Negro Ponzi, M.M., Aceto, M., 2008. ICP–MS analysis of glass fragments of Parthian and Sasanian epoch from Seleucia and Veh Ardaŝīr (central Iraq). Archaeometry 50, 429–450.
Phelps, M., 2017. An Investigation Into Technological Change and Organisational Developments in Glass Production between the Byzantine and Early Islamic Periods (7th–12th Centuries) Focussing on Evidence From Israel. PhD thesis. University of London.
Phelps, M., 2018. Glass supply and trade in early Islamic Ramla: an investigation of the plant ash glass. In: Rosenow, D., Phelps, M., Meek, A., Freestone, I.C. (Eds.), Things that Travelled: Mediterranean Glass in the First Millennium CE. UCL Press, London, pp. 236–282.
Rante, R., 2008. The Iranian city of Rayy: urban model and military architecture. Iran 46, 189–211.
Rante, R., 2015. Rayy: From Its Origins to the Mongol Invasion: An Archaeological and Historiographical Study, Brill, Leiden.
Salehvand, N., Agha-Aligol, D., Shishegar, A., Rachti, M.L., 2020. The study of chemical composition of Persian glass vessels of the early Islamic centuries (10th– 11th centuries AD) by micro-PIXE; case study: Islamic collection in the National Museum of Iran. J. Archaeol. Sci. Rep. 29, 102034.
Schibille, N., 2022. Islamic Glass in the Making: Chronological and Geographical Dimensions. Leuven University Press, Leuven.
Schibille, N., Gratuze, B., Ollivier, E., Blondeau, É., 2019. Chronology of early Islamic glass compositions from Egypt. J. Archaeol. Sci. 104, 10–18.
Schibille, N., Meek, A., Wypyski, M.T., Kröger, J., Rosser-Owen, M., Haddon, R.W., 2018. The glass walls of Samarra (Iraq): ninth-century Abbasid glass production and imports. PLoS One 13, e0201749.
Shortland, A., Rogers, N., Eremin, K., 2007. Trace element discriminants between Egyptian and Mesopotamian Late Bronze Age glasses. J. Archaeol. Sci. 34, 781–789.
Swan, C.M., Rehren, Th., Lankton, J., Gratuze, B., Brill, R.H., 2017. Compositional observations for Islamic glass from Sīrāf, Iran, in the Corning Museum of Glass collection. J. Archaeol. Sci. Rep. 16, 102–116.
Wilkinson, C.K., 1973. Nishapur: Pottery of the Early Islamic Period. Metropolitan Museum of Art, New York.
Wypyski, M.T., 2015. Chemical analysis of early Islamic glass from Nishapur. J. Glass Stud. 57, 121–136.